Systematic monitoring of photosynthetically-derived oxidative signals using a 2-Cys peroxiredoxin-based redox probe

Nardy Lampl[1], Idan Nissan[1], Gal Gilad[1], Matanel Hipsch[1] and Shilo Rosenwasser[1]

[1]The Robert H. Smith Institute of Plant Sciences and Genetics in Agriculture, The Hebrew University, Rehovot, Israel

* Corresponding author. email: shilo.rosenwaser@mail.huji.ac.il (SR)

Abstract

Transmission of reductive and oxidative cues from the photosynthetic electron transport chain to redox regulatory protein networks plays a crucial role in coordinating chloroplast metabolism and photosynthetic activities. The tight balance between these two signals dictates the cellular response to changing light conditions. The highly abundant stromal peroxidase, 2-Cys peroxiredoxin (2-Cys Prx), derives light-dependent oxidative signals by transferring oxidizing equivalents of photosynthetically produced H_2O_2 to redox-regulated proteins. However, a comprehensive physiological understanding of the role of oxidative signals under changing light intensities is still lacking, mainly due to the difficulties in accurately and nondestructively monitoring them. Here, we introduced chl-roGFP2-PrxΔC_R, a 2-Cys Prx-based biosensor, into *Arabidopsis thaliana* chloroplasts to monitor the dynamic changes in photosynthetically-derived oxidative signaling. We showed that chl-roGFP2-PrxΔCR oxidation states reflected the similar oxidation patterns of endogenous 2-Cys Prx under varying light conditions, as determined by both redox western blots and fluorescence measurements. Furthermore, systematic monitoring of probe oxidation throughout the day led to the identification of the dynamic light intensity range of 2-Cys Prx-mediate redox signaling and demonstrated the induction of quantifiable redox signals under low-light conditions. The presented data highlights the role of oxidative signals under nonstressed conditions and suggests 2-Cys Prx-based biosensor as a powerful tool to explore their dynamic in higher plants.

Introduction

Sophisticated mechanisms enabling adjustments of light-capturing reactions and downstream metabolic processes have evolved in sessile plants, allowing them to reach optimal photosynthetic performance. Under low-light conditions, efficient photosynthetic activity and tight regulation of the reducing power distribution between essential metabolic pathways are required for optimal utilization of the available energy input. On the other hand, energy dissipation under high-light (HL) conditions is critical to avoid over-production of harmful reactive oxygen species (ROS) (Asada, 2006). Reductive and oxidative signals, both emanating from the photosynthetic electron transport chain (PETC), and their transfer to regulated thiol proteins, play a significant role in linking the performance of photosynthesis to chloroplast transcription, translation, and metabolic processes, thereby enabling rapid acclimation to instantaneous changes in daytime photon fluxes (Schürmann and Buchanan, 2008; Buchanan and Balmer, 2005; Dietz and Pfannschmidt, 2011; Scheibe and Dietz, 2012; Foyer and Noctor, 2009).

Reductive signals in chloroplasts are mainly generated by the flux of electrons derived from ferredoxin, via ferredoxin-dependent thioredoxin reductase (FTR), to thioredoxins (Trxs) (Schürmann and Buchanan, 2008) and via NADPH-dependent thioredoxin reductases C (NTRC) (Serrato et al., 2004), thereby linking chloroplast metabolism to light availability and photosynthetic activity. Counteracting oxidative signals are mainly generated from electron flux through the water-water cycle (WWC). During the WWC, electrons are donated from photosystem I (PSI) to molecular oxygen in the Mehler reaction, yielding superoxide radicals ($O_2^{\cdot-}$), which are then dismutated to molecular oxygen (O_2) and H_2O_2 in a reaction catalyzed by superoxide dismutase (SOD) (Mehler, 1951; Rizhsky et al., 2003; Mittler et al., 2004). The production of H_2O_2 through the WWC allows communication between the photosynthetic light reactions and downstream metabolic processes by transmitting oxidative signals to redox-regulated proteins (Apel and Hirt, 2004; Mullineaux et al., 2018; Smirnoff and Arnaud, 2019).

The detoxification of photosynthetically produced H_2O_2 is mediated by chloroplast-targeted ascorbate peroxidases (APXs) and 2-Cys peroxiredoxins (2-Cys Prxs) (Dietz, 2016; Awad et al., 2015). The latter are highly abundant and remarkably efficient thiol peroxidases, displaying high catalytic efficiency of up to 10^8 M^{-1} s^{-1} (König et al., 2002; Dietz et al., 2006). Electrons delivered from the PETC, reduce 2-Cys Prx via the FTR/TRX pathways or through NADPH via NTRC activity (Pulido et al., 2010; Collin et al., 2003; Pérez-Ruiz and Cejudo, 2009; Cerveau et al.,

2016). Therefore, the 2-Cys Prxs redox state is determined by the balance between photosynthetically produced reducing and oxidizing equivalents. Importantly, recent studies have demonstrated oxidative signal transmission, mediated by 2-Cys Prxs, from H_2O_2 to target proteins, at the onset of the light and dark periods and under low- and fluctuating-light conditions (Dangoor et al., 2012; Eliyahu et al., 2015; Vaseghi et al., 2018; Ojeda et al., 2018; Yoshida et al., 2018). Despite the considerable importance of the regulatory role of 2-Cys Prx, most of our current knowledge is based on measuring its oxidation state using western blot analysis or examination of mutant lines performance, rendering it challenging to detect the transmission of oxidative signals in real-time and with high temporal resolution.

Genetically encoded redox-sensitive green fluorescent protein (roGFP) probes enable, due to their high sensitivity and reversibility, systematic *in vivo* mapping of H_2O_2 production and the glutathione redox state (E_{GSH}), in different sub-cellular compartments (Dooley et al., 2004; Hanson et al., 2004; Jiang et al., 2006; Meyer et al., 2007; Gutscher et al., 2008; Meyer and Dick, 2010; Nietzel et al., 2019; Gutscher et al., 2009). In vitro characterization of roGFP showed that its reduction is mediated by Glutaredoxins (Grxs), which catalyze the reversible electron flow between GSH and target proteins (Gutscher et al., 2008; Meyer et al., 2007). Recently, an H_2O_2 sensor based on a redox relay mechanism between Tsa2, a highly efficient *S. cerevisiae* 2-Cys peroxiredoxin, and roGFP2 was developed (Morgan et al., 2016). To increase the probe's sensitivity to low H_2O_2 levels, a mutation in the resolving cysteine (C_R) of Tsa2 (roGFP2-Tsa2ΔC_R) was introduced, thus preventing competition between the Trx-mediated reduction of the Tsa2 moiety and roGFP oxidation. The resulting probe enabled the measurement of endogenous basal H_2O_2 levels in yeast (Morgan et al., 2016) and *Chlamydomonas reinhardtii* cells (Niemeyer et al., 2020); however, such a roGFP2 Prx-based probe has not been yet implemented to measure the dynamic oxidation of 2-Cys Prx in higher plants.

Here, we employed chl-roGFP2-PrxΔC_R, a new 2-Cys Prx biosensor, to establish the role of 2-Cys Prx in light-dependent oxidative signal transmission in *Arabidopsis* plants. By parallel measurements of the endogenous 2-Cys Prx and chl-roGFP2-PrxΔC_R oxidation states, we showed that 2-Cys Prx is directly regulated by light intensity. Furthermore, the dynamics of 2-Cys Prx-dependent oxidative signals, throughout the day, under various light conditions, were resolved by systematic monitoring of the probe's redox state. Determination of the light intensity range of 2-

Cys Prx-mediated redox signaling suggests its role in redox signaling under habitual conditions rather than oxidative stress.

Results

The oxidation state of chloroplastic 2-Cys Prx is firmly linked to changes in light intensities

To explore the effect of light intensity on the redox state of 2-Cys Prx, wild-type *Arabidopsis* plants were exposed to HL (600 or 1000μmol photons m^{-2} s^{-1}) or to normal growth light conditions (GL, 120 μmol photons m^{-2} s^{-1}). The 2-Cys Prx redox state was then monitored *in planta* by redox western blot analysis (Fig. 1). To retain the *in vivo* thiol oxidation status of 2-Cys Prx, protein extracts were prepared in the presence of trichloroacetic acid (TCA), and thiols were irreversibly blocked with N-ethylmaleimide (NEM) under non-reducing conditions. The higher and the lower molecular weight bands represent the oxidized dimer and reduced monomer forms, respectively (Fig. 1). In agreement with a previous report (Dangoor et al., 2012), transferring plants from dark to GL resulted in a reduction of 2-Cys Prx, as reflected by the dominance of the dimer band under dark conditions (~75% of total Prx was oxidized) and by the decrease in its relative abundance under light conditions (~55% oxidized, Fig. 1A&B). Importantly, this reduction was not observed in plants that were pretreated with 3-(3,4-dichlorophenyl)-1,1-dimethylurea (DCMU), an inhibitor of photosynthetic electron transport (Fig 1A&B), simulating dark conditions. Interestingly, when plants were exposed to HL intensities (600 or 1000 μmol photons m^{-2} s^{-1}), 2-Cys Prx was reduced upon dark to light transition but stabilized at a higher oxidation state, as compared with GL, with no significant difference in its redox state between the two examined high-light intensities (Fig. 1A&B).

The observed 2-Cys Prx dimers represent two possible oxidation states, i.e., the fully-oxidized (2S-S) and half-oxidized (1S-S) forms. A gel-shift assay carried out with methoxypolyethylene glycol-maleimide (mPEG) to distinguish between these two oxidation states, identified three bands, with the higher and the middle bands corresponding to the fully-oxidized (2S-S) and half oxidized (1S-S) forms, respectively (Fig. 1C&D). Under dark conditions, a relatively high level of the fully-oxidized form was observed. On transfer of plants from dark to GL, the relative levels of the fully reduced form significantly increased and were paralleled by a decrease in the fully-oxidized form. Such a reduction was not detected in plants treated with DCMU under GL. Plants

transferred to 600µmol photons m^{-2} s^{-1} showed a slight decrease in the relative amount of the fully reduced form as compared to plants grown under GL. A significant amount of fully oxidized 2-Cys Prx was observed in plants exposed to 1000 µmol photons m^{-2} s^{-1} (Fig. 1C&D), suggesting that increased illumination enhanced 2-Cys Prx dimer formation, in which both catalytic sites participate in disulfide exchange reactions.

To explore the dynamics of the 2-Cys Prx redox state under prolonged, physiologically relevant light conditions, we further examined the 2-Cys Prx redox state throughout the day, while plants were exposed to gradually increasing light intensities, reaching a maximum value of 900 µmol photons m^{-2} s^{-1}, followed by a gradual decrease in light intensities toward the dark period (Fig. 1E&F). *Arabidopsis* wild-type plants were sampled approximately every hour, and the relative abundance of the dimers (oxidized) and monomers (reduced) was determined. An apparent light-dependent response of the 2-Cys Prx redox state was observed. The most reduced form of 2-Cys Prx was observed under low-light levels, at the beginning and the end of the day, while the most oxidized state was observed in the middle of the day when the light intensity reached a maximum level. Interestingly, the major shift in oxidation was during the transition from low (80-130 µmol photons m^{-2} s^{-1}) to moderate (240-280 µmol photons m^{-2} s^{-1}) light intensities, at the initiation and termination of the light phase (Fig.1 E&F). No detectable Prx hyperoxidation was observed (Fig. 1F). To summarize, these observations demonstrated that the 2-Cys Prx redox state is directly affected by the PETC and that its oxidation state is dependent on light intensity.

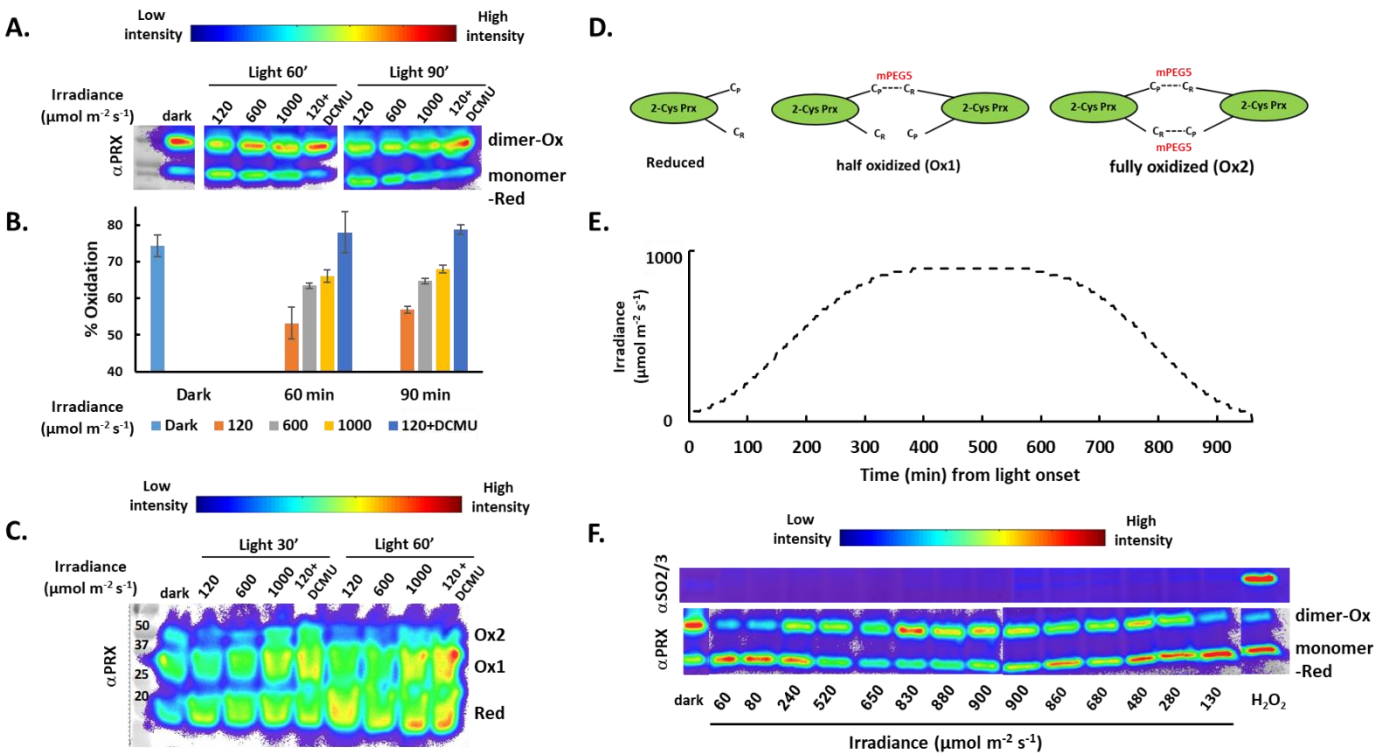

Figure 1: Light responsiveness of the 2-Cys Prx redox state. (A) An immunoblot showing the oxidized and reduced states of 2-Cys Prx, as dimers and monomers, respectively. Plants were kept in the dark for 8 h and then exposed for 5.5 h to the indicated light intensities. Total protein was extracted using trichloroacetic acid (TCA), and free thiols were blocked with N-ethylmaleimide (NEM). (B) Quantification of the immunoblot bands shown in A. (C) Gel-shift assay with mPEG showing the in vivo redox state of 2-Cys Prx residues in plants exposed to light intensities as in A. NEM treatment was applied to block reduced thiols and DTT to reduce disulfides before mPEG labeling. The number of oxidized Cys residues (Ox1 and Ox2) was determined by the increased molecular mass of 2-Cys Prx after labeling with mPEG. (D) Schematic illustration of the redox mobility gel assay. (E) Light intensity over time. (F) Plants were exposed to the light regime indicated in E. Immunoblot assay showing the oxidized and reduced states of 2-Cys Prx, as dimer and monomer, respectively and the hyperoxidiezed form, so2/3. *for additional time points for A&C see Supp. Fig. 1.

Developing a genetically encoded chloroplast-targeted roGFP2-PrxΔC_R

The observed light sensitivity of 2-Cys Prx motivated us to develop a chloroplast-targeted fluorescent protein-based reporter to facilitate nondestructive and real-time measurements of oxidative signals transmitted to target proteins through 2-Cys Prx under variable light conditions. To this end, we generated the chl-roGFP2-PrxΔC_R probe by genetically fusing roGFP2 to a mutated version of 2-Cys Prx A (BAS1), in which the resolving cysteine (C_R) was changed to alanine (Fig. 2A). Chloroplast targeting was achieved using the BAS1 signal peptide and verified by the overlapping of the roGFP2 fluorescence and chlorophyll fluorescence signals (Fig. 2B). The formation of intact fused probes was verified by SDS-PAGE and western blotting using either anti-PRX or anti-GFP antibodies (Fig. 2C). Blotting with anti-PRX showed lower expression level of the probe as compared to endogenous 2-Cys Prx, ensuring minimal interference with the endogenous redox metabolism and antioxidant activity. BAS1 was fused at its N terminus to roGFP2, since initial attempts to fuse it at its C terminus resulted in probe cleavage (Supp. Fig. 2). Interestingly, the cleaved roGFP obtained from the fusion of BAS1 at its C-terminus was localized in the chloroplast (Supp. Fig. 2), suggesting that the C terminus of BAS1 is prone to cleavage by specific chloroplast proteases. To calibrate the probe dynamic range, 3-week-old plants grown in soil were soaked with H_2O_2 or DTT and probe emission at 515 nm was recorded using a fluorescence plate reader, following excitation at 405 and 465nm. Ratio values (R) obtained from the emitted fluorescence division due to excitation at 405nm versus 465nm indicated the roGFP2 oxidation state (Hanson et al., 2004; Dooley et al., 2004). As shown in Fig. 2D, a dynamic range of 5.6 was calculated between the fully oxidized (R_{oxi}=0.45) and fully reduced ($R_{red=}$0.08) forms, ensuring a sufficient signal to noise ratio. chl-roGFP2-PrxΔC_R was more oxidized compared with chloroplast-targeted roGFP2 (chl-roGFP2) at steady-state (~65% and ~40%, respectively), confirming the effect of BAS1 moiety on roGFP2 redox state and in agreement with the high oxidation state of roGFP2-Tsa2ΔC_R in yeast (Morgan et al., 2016).

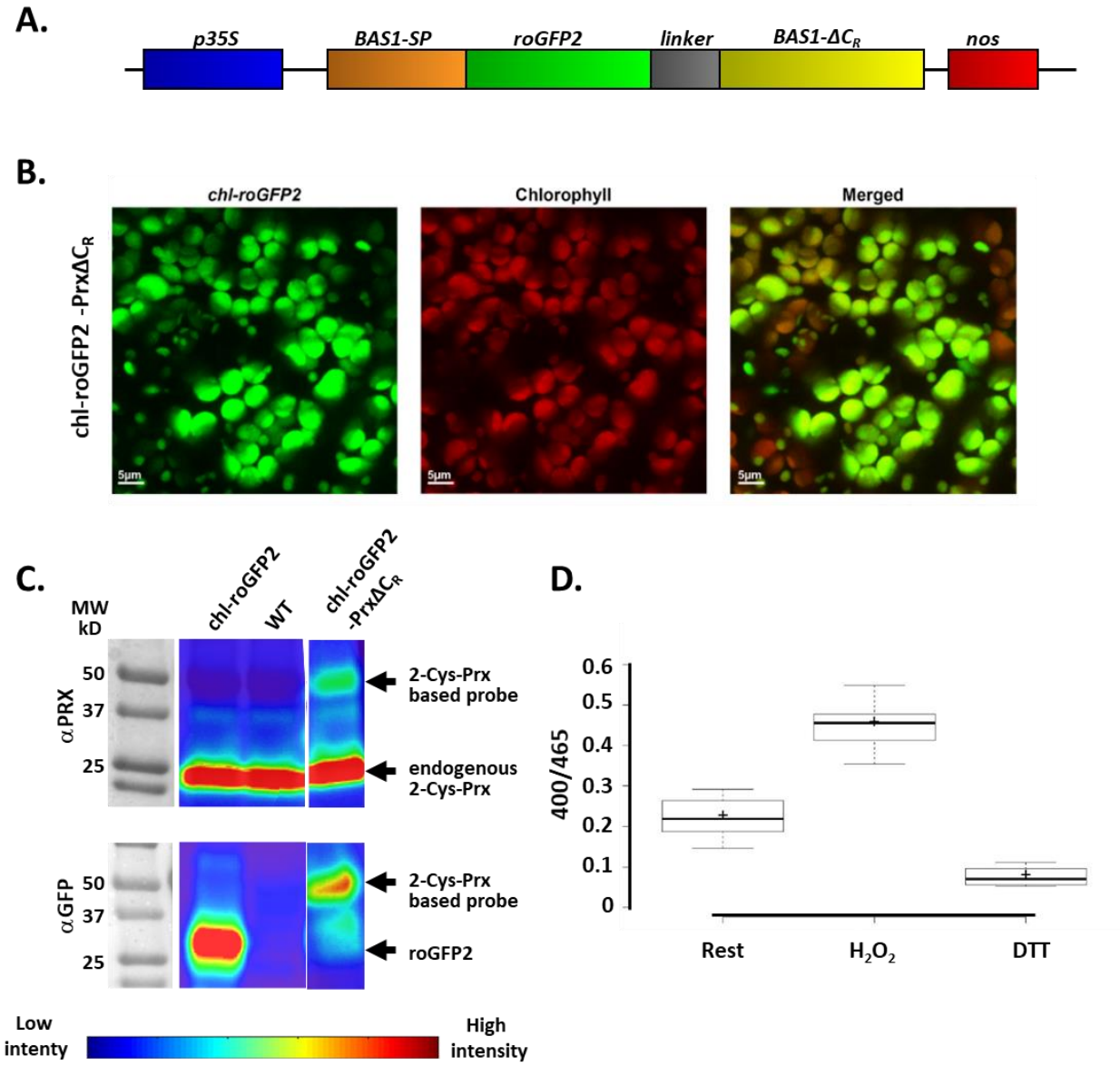

Figure 2: Chloroplast-targeted peroxiredoxin-based redox probes. (A) Schematic diagram of the gene cassette used to transform Arabidopsis plants. (B) Subcellular localization of chl-roGFP2-PrxΔCR in mesophyll cells, as detected by confocal microscopy. (C) In vivo detection of the fused sensor protein by western blot analysis using either anti-Prx or anti-GFP antibodies. (D) Fluorescence ratio (405/465) in plants expressing chl-roGFP2 or chl-roGFP2-PrxΔC_R under steady-state conditions and following treatment with 100mM DTT or 500mM H_2O_2. The emitted fluorescence from three-week-old plants grown in soil was recorded using a plate reader.

The oxidation state of chloroplast-targeted roGFP2-PrxΔC_R is light-sensitive

Having established the light dependency of the 2-Cys Prx redox state (Fig. 1), we sought to examine the probe sensitivity to light intensity by monitoring the oxidation degree of chl-roGFP2-PrxΔC_R in comparison to the chl-roGFP2 during dark to light transition. Experiments were conducted by exposing dark-adapted plants expressing both probes to 5 min of light; fluorescence signals were recorded using a highly sensitive *in vivo* imaging system. Whole-plant ratiometric analysis showed that the chl-roGFP2-PrxΔC_R probe was ~ 60% oxidized under steady-state conditions (Fig. 3), matching the observations obtained by the fluorescence plate reader approach (Fig. 2D). Remarkably, significant changes were observed in the oxidation degree (OxD) of chl-roGFP2-PrxΔC_R upon shifting plants from dark to different light intensities (450, 750, or 1000 µmol photons m^{-2} s^{-1}) (Fig. 3). Moreover, chl-roGFP2-PrxΔC_R reached its almost fully oxidized state, within 5 min of transition from dark to the examined light intensities (Fig. 3A&C). In contrast, the unfused chl-roGFP2 probe was only moderately oxidized under these conditions (Fig. 3A&B). These findings demonstrate the enhanced light sensitivity of chl-roGFP2-PrxΔC_R compared to the chl-roGFP2, achieved by positioning BAS1 in close proximity to roGFP2. Moreover, as both probes are subjected to reduction in a GSH/GRX-dependent manner, the comparison between their dynamic oxidation allows resolving the effect to H_2O_2-dependent thiol oxidases mediated by BAS1.

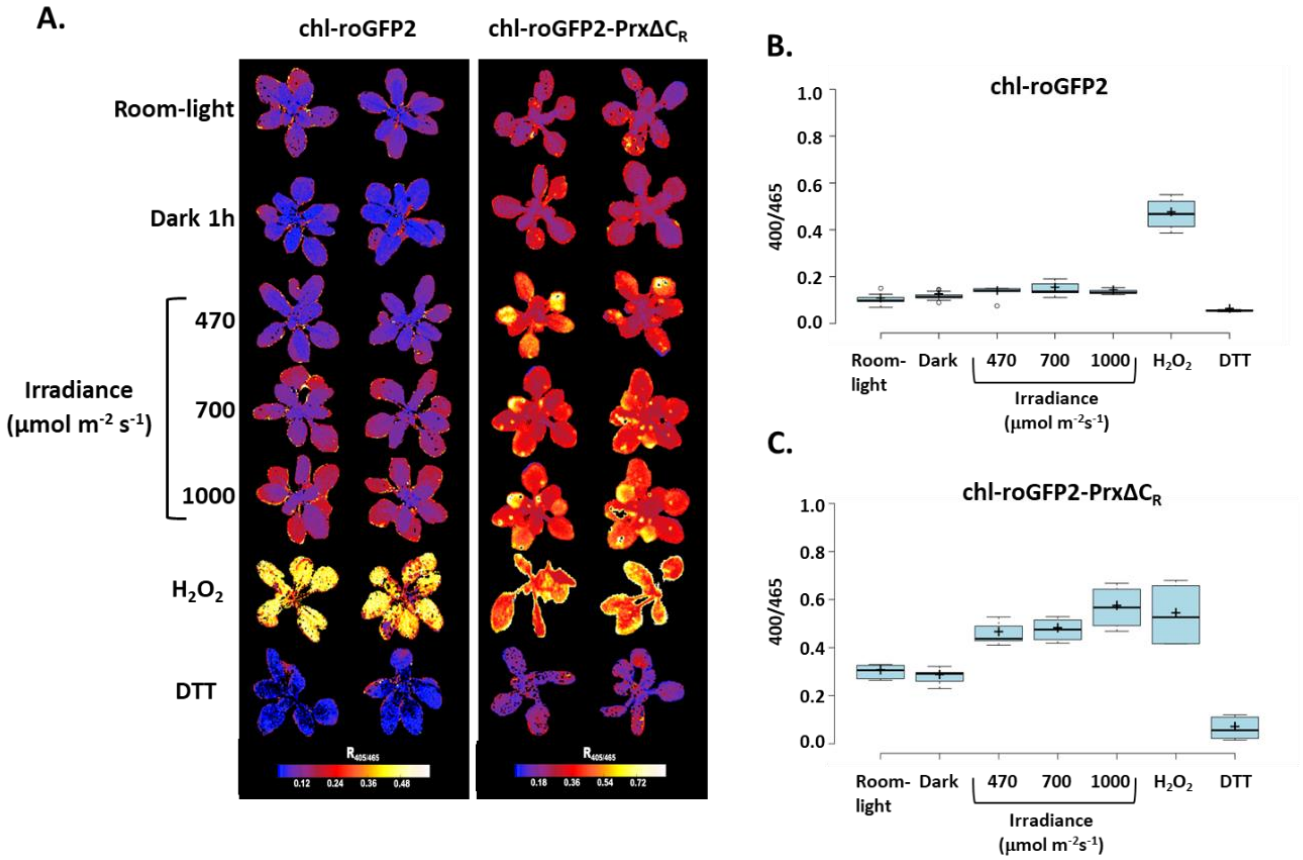

Figure 3. Whole-plant fluorescence imaging of plants expressing chl-roGFP2 or chl-roGFP2-PrxΔC$_R$ during dark to light transitions. (**A**) Whole-plant ratiometric analysis of chl-roGFP2 and chl-roGFP2-PrxΔC$_R$ fluorescence during resting state (ambient light), after 1 h in dark and 5 min after transfer from darkness to different light intensities. In addition, ratiometric analysis following treatments with 100mM DTT or 500mM H_2O_2 are presented. The roGFP2 fluorescence images were captured at 510 nm, following excitation at 400 nm and 465 nm. Ratiometric analysis (400/465) was performed via Matlab in false color. (B) and (C) Quantification of ratiometric images presented as box-plots. For the quantification, autofluorescence of wild-type plants was deducted from the total fluorescence detected from the transgenic plants.

The responsiveness of chl-roGFP2-PrxΔC_R matched the low-moderate light intensity range

We further investigated the daily dynamics of the chl-roGFP2-PrxΔC_R oxidation state using an automated system that allows for continuous measurements of roGFP-based signals (Haber and Rosenwasser, 2020). Measurement of chl-roGFP-PrxΔC_R OxD was conducted in plants exposed to GL (120 μmol photons m^{-2} s^{-1}) and same HL conditions (600 or 1000 μmol photons m^{-2} s^{-1}) as in Fig1A&B, during a 16 h light/8 h dark cycle. While probe oxidation was detected upon transition from dark to light under all examined light conditions, significantly higher oxidation values were recorded in plants under HL (~85-95%) than GL (~65-70 %; Fig. 4A). No significant differences in probe oxidation degree were observed between plants exposed to 600 or 1000 μmol photons m^{-2} s^{-}. Notably, oxidation values were stable throughout the entire light period, and probe reduction was observed only when the light was turned off. These results, which point to the differential stabilization of chl-roGFP-PrxΔC_R redox state in plants exposed to GL and HL, were in agreement with the oxidation state of endogenous 2-Cys Prx, as measured by western blot analysis (Fig. 1A&B and Supp. Fig. 1), supporting the notion that the probe redox state is determined by oxidizing equivalents received from H_2O_2 through 2-Cys Prx.

A comparison between the redox state of the chl-roGFP2-PrxΔC_R and chl-roGFP2 probes under these conditions revealed distinct patterns. While oxidation values of chl-roGFP2-PrxΔC_R were stable during the light period, chl-roGFP2 underwent oxidation followed by reduction, upon dark-light transition, with OxD values being even slightly lower than those seen in the dark after plant exposure to GL (Supp. Fig. 3). These results further point to the higher sensitivity of chl-roGFP2-PrxΔC_R to light and demonstrate its effective and continuous real-time tracking of 2-Cys Prx-mediated oxidative signals in intact plants throughout the entire day.

To compare the oxidation dynamics of chl-roGFP2-PrxΔC_R to that of chl-roGFP2 under a range of light intensities, their OxD was continuously monitored in plants exposed to gradual changes in light intensities, as described in Fig.1F. As shown in Fig. 4B, entirely different oxidation patterns were observed between the two probes. Interestingly, the chl-roGFP2-PrxΔC_R OxD sharply increased from the light onset, reaching its full oxidation state after approximately two hours, when the light intensity was ~300 μmol m^{-2} s^{-1}. A gradual reduction in OxD was observed only at 14 h after light onset, when light intensities were dimmed again. In contrast, the chl-roGFP2 OxD gradually increased, reaching its highest level (65%) after 3 h, when the light intensity was ~600 μmol m^{-2} s^{-1}. From this point onward, a gradual decrease in chl-roGFP2

oxidation was observed, reaching its lowest oxidation degree (42%) at the beginning of the dark period. Differential oxidation patterns were also observed during the dark period; while the chl-roGFP2-PrxΔC$_R$ OxD was constant, a reduction followed by gradual oxidation was observed for chl-roGFP2. The similar light-responsive range of chl-roGFP2-PrxΔC$_R$ probe (Fig. 4B) and endogenous 2-Cys Prx (Fig.1E) support the probe specificity for the 2-Cys Prx redox state.

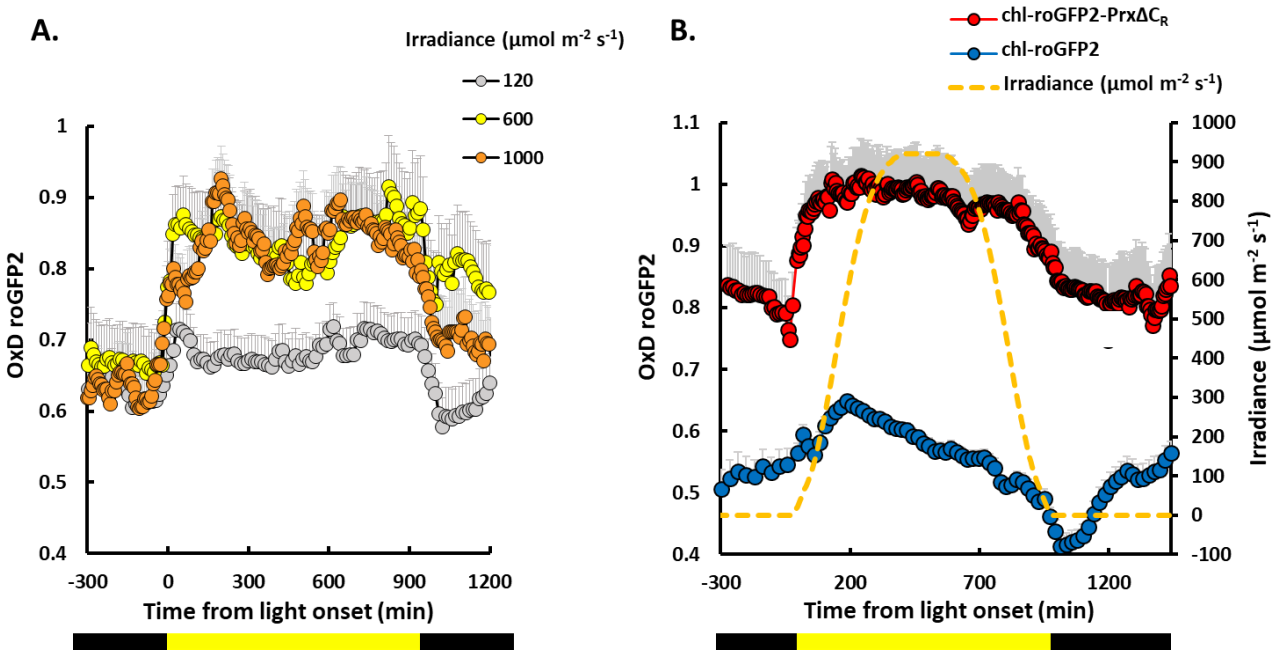

Figure 4: Systematic monitoring of light-induced oxidative signals. Daily changes in oxidation degree (OxD) in 3-week-old plants grown in 12-well plates, were measured. For each line, between 24 and 40 plants divided into 3-5 independent plates were analyzed and consolidated in a "sliding window" (n=3-5) display. Values represent means ± SE. The color bar denoted the light conditions: black-darkness, yellow-light. (A) Dynamic changes in chl-roGFP2-PrxΔC$_R$ OxD in plants exposed to growth light (GL) (120µmol photons m^{-2} s^{-1}) or high light (HL) (600 or 1000µmol photons m^{-2} s^{-1}) after 8 h in the dark. (B) A comparison between chl-roGFP2 and chl-roGFP2-PrxΔCR OxD throughout the day is presented. The applied light intensities are depicted as a dashed yellow line.

chl-roGFP-PrxΔC$_R$ uncovers low-light-induced oxidative signals

The increasing recognition that oxidative signals play a dominant role in fine-tuning of metabolic activity under low-light conditions (Dangoor et al., 2012; Eliyahu et al., 2015; Vaseghi et al., 2018; Wolf et al., 2020), drove us to further investigate the sensitivity of the chl-roGFP2-PrxΔC$_R$ redox state in the transition from dark to low light. To this end, we exposed dark-adapted chl-roGFP2-PrxΔC$_R$ and chl-roGFP2 plants to low light (~22 µmol photons m^{-2} s^{-1}) for several hours. Strikingly, the two probes showed contrasting responses upon transition from dark to low light (Fig. 5A). While chl-roGFP2-PrxΔC$_R$ OxD slightly increased when plants were transferred

to low light, chl-roGFP2 OxD underwent a significant reduction. This reduction continued for at least 2 hours from light onset until stabilization at a lower degree of oxidation (35%). To better characterize probe responsiveness to the low-light intensity range, plants were then exposed to a gradual increase in light intensities, starting with ~22 µmol photons m^{-2} s^{-1} and increasing up to 330µmol photons m^{-2} s (Fig. 5B). An immediate reduction of chl-roGFP2 was observed at ~22 µmol photons m^{-2} s^{-1}, followed by oxidation at a light intensity of ~44 µmol photons m^{-2} s^{-}, with oxidation reaching a maximum under 330µmol photons m^{-2} s^{-1}. In contrast, gradual oxidation of chl-roGFP-PrxΔC_R was observed with progress through the low-light gradient. Interestingly, when the light intensity was decreased (at 600 min), a similar reduction pattern was observed for both probes, indicating a minor effect on the 2-Cys Prx moiety on probe reduction dynamics. The opposite response of the two probes at the onset of low-light demonstrates real-time *in vivo* tracking of the activation of counterbalanced oxidative and reductive signals mediated by 2-Cys Prx and GSH/GRXs, respectively.

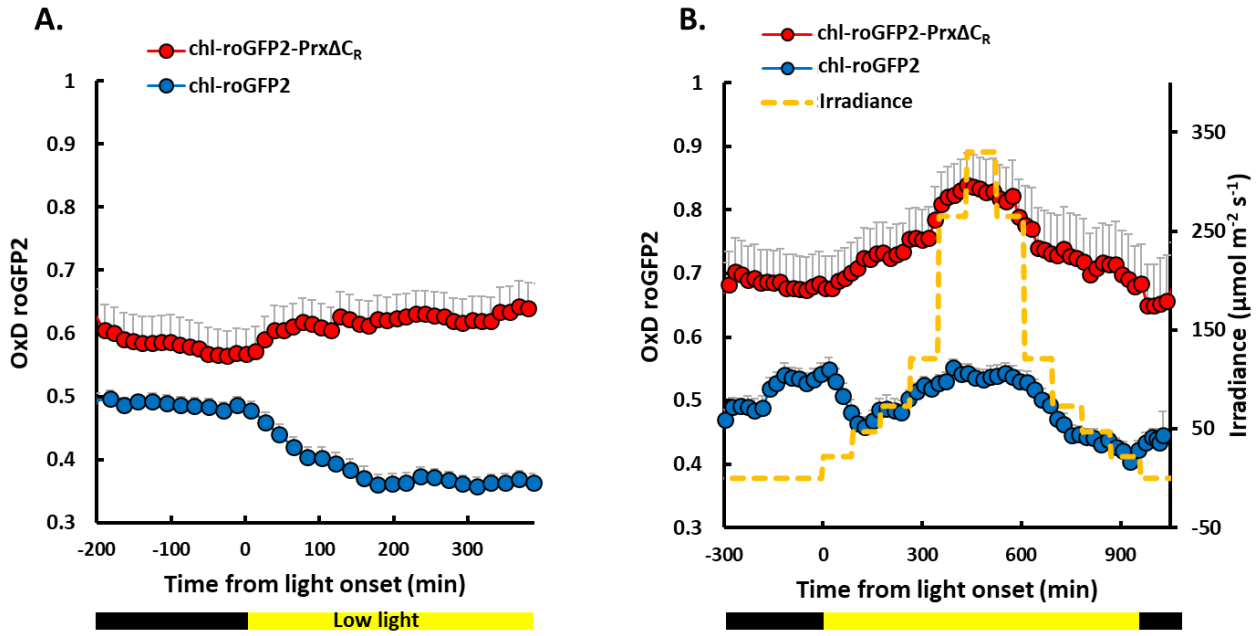

Figure 5: chl-roGFP2-PrxΔC_R demonstrates the induction of oxidative signals under low light. Presented is a comparison between chl-roGFP2 and chl-roGFP2-PrxΔC_R oxidation degree (OxD), monitored in 3-week-old plants grown in 12-well plates. For each line, between 24 and 40 plants divided into 3-5 independent plates were analyzed and consolidated in a "sliding window" (n=3-5) display. Values represent means ± SE. The color bar denoted the light conditions: black-darkness, yellow-light. (A) Dynamic changes in chl-roGFP2 and chl-roGFP2-PrxΔC_R OxD at the onset of low light (22µmol photons m^{-2} s^{-1}). (B) Daily dynamic changes in chl-roGFP2 and chl-roGFP2-PrxΔC_R OxD in plants exposed to a gradual increase from low to moderate light intensities, followed by an equivalent decrease. The applied light intensities are depicted as a dashed yellow line.

Discussion

In addition to their antioxidant activity (Awad et al., 2015), chloroplast-targeted 2-Cys Prx is now recognized to mechanistically link photosynthetically produced H_2O_2 and chloroplast redox metabolism by transmitting, through their thioredoxin oxidase activity, oxidative equivalents to target proteins (Dangoor et al., 2012; Eliyahu et al., 2015; Vaseghi et al., 2018; Yoshida et al., 2018; Pérez-Ruiz et al., 2017). The central role of 2-Cys Prx in redox signaling prompted us to establish a redox biosensor that will allow for nondestructive real-time measurement of 2-Cys Prx-based oxidative signals. The capability of cellular peroxidases to transfer oxidative equivalents to genetically linked roGFP2 provided a mechanistic framework for developing H_2O_2-specific redox probes (Stöcker et al., 2017; Gutscher et al., 2009; Nietzel et al., 2019; Morgan et al., 2016). Among these probes is the 2-Cys peroxiredoxin (Tsa2)-based roGFP2 that was developed in *S. cerevisiae*. A significant enhancement of probe sensitivity was achieved by substituting the resolving cysteine of Tsa2 by alanine, impeding its TRX-dependent reduction (Morgan et al., 2016).

On this basis, we established the chloroplast-targeted roGFP2-PrxΔC_R probe by genetically fusing roGFP2 to a mutated version of 2-Cys Prx A (BAS1) in *Arabidopsis* plants. Notably, the relatively low levels of roGFP2-PrxΔC_R (Fig. 2B) compared to the highly abundant endogenous 2-Cys Prxs (König et al., 2002) suggests a negligible interfering effect of the engineered probe with natural stromal H_2O_2 metabolism. Despite the high sensitivity of the chl-roGFP2-PrxΔC_R to H_2O_2, achieved by eliminating the reduction power reached from FTR/Trx and NTRC, the changes in probe oxidation state cannot merely be interpreted as a reflection of changes in stromal H_2O_2 concentrations, as the actual probe oxidation state is also affected by the rate of its reduction by the GSH/GRXs system. Accordingly, the oxidative activity of 2-Cys Prx can only be assessed by comparing the oxidation state of the chl-roGFP2-PrxΔC_R to that of the unfused chl-roGFP2.

The presented comparison between the oxidation state of chl-roGFP2-PrxΔC_R and chl-roGFP2 demonstrated differential responses to light and displayed the unique attributes of roGFP2-PrxΔC_R in tracking oxidative signals. More specifically, the stabilization of the roGFP2-PrxΔC_R probe at a higher oxidation state than the chl-roGFP2 under steady-state conditions, a phenomenon also observed with the roGFP2-Tsa2ΔC_R probe (Morgan et al., 2016; Niemeyer et al., 2020), indicates a direct effect of 2-Cys Prx on the roGFP moiety. In addition, the stable

oxidation of roGFP2-PrxΔC_R observed upon plant transfer from dark to normal GL conditions of 120 µmol m^{-2} s^{-1} suggests that its oxidation rate by 2-Cys Prx during dark-light transition exceeds its rate of reduction by GSH/GRXs. A contrasting effect was observed in the chl-roGFP2 probe, for which the rate of reduction outcompeted the rate of oxidation, as indicated by the peak in oxidation followed by reduction upon dark to light shift (Supp. Fig. 3, Haber and Rosenwasser, 2020). Furthermore, the almost fully oxidized state of roGFP2-PrxΔC_R under HL, compared with the more reduced state of the chl-roGFP2 under similar light conditions further point for its enhanced light sensitivity (Supp. Fig.3 ,Haber and Rosenwasser, 2020). Moreover, the oxidation dynamics of both probes throughout the day, in response to a gradual increase, followed by a gradual decrease in light intensities, revealed a particular light intensity sensitivity range for the-roGFP2-PrxΔC_R that matched the light intensities sensitivity range shown for 2-Cys Prx (Fig. 1F and Fig. 4B). Most strikingly, the relatively stable oxidation state of roGFP2-PrxΔC_R after the onset of low light compared to the reduction observed in the chl-roGFP2 under these same conditions, suggest the induction of oxidative signals under low-light intensities, attenuating the reductive signals emanated from GSH/GRXs activity. These results matched the increasingly recognized role of 2-Cys Prx in adjusting photosynthetic activity and chloroplast metabolism under low and fluctuating light conditions, as revealed in recent biochemical and genetic studies. While 2-Cys Prx redox signaling is prevalent under low-moderate light intensities, under severe HL conditions, in which a higher rate of peroxide production is expected, the antioxidant activity rather than the signaling role of 2-Cys Prx, is dominant, as indicated by increases in the fully-oxidized 2-Cys Prx state (2S-S, Fig. 1C, Supp.Fig.1).

The observed strong link between the redox state of the endogenous 2-Cys Prx and the redox state of roGFP2-PrxΔC_R in response to changes in light intensities (compare Fig. 1F to Fig. 4B) suggests that it may serve as a high-precision tool to track the in vivo state of 2-Cys Prx in living plants. These results fit the dominant role of endogenous 2-Cys Prx in driving the oxidation of the yeast roGFP2-Tsa2ΔCR probe (Morgan et al., 2016). Interestedly, the correlation between the probe and endogenous 2-Cys Prx oxidation was not detected at night; while the probe exhibited its most reduced state, 2-Cys Prx was at its most oxidized state. As shown by Morgan et al., (2016), roGFP2-Tsa2ΔCR integrates into endogenous Tsa decamers. Destabilization of the reduced decamers was suggested to occur upon oxidation and formation of disulfides, resulting in the unbound oxidized dimer and decrease in peroxidase activity (Nelson et al., 2018). In addition, no

decamers were found in plants under dark (König et al., 2002). Thus, it is possible that the observed highly oxidized state of endogenous 2-Cys Prx under dark conditions (Fig. 1D) is accompanied with oligomer destabilization and a decrease in probe reactivity toward peroxides. Under such conditions, the GSH/GRXs pathway activity is dominant, resulting in its higher reduced state (Fig 4&5). The observed reduction of the oxidized dimers at the onset of the light period (Fig 1D) suggests reforming the reduced oligomers and increased peroxidase activity, which results in increase of roGFP2-PrxΔC_R sensitivity toward oxidation (Fig 4&5). It is possible that unknown chloroplastic factor block oligomerization during dark keeping 2-Cys Prx and roGFP2-PrxΔCR in a less catalytically active state. Future investigations of 2-Cys Prx oligomerization dynamics in plants during the light-dark transition, possibly using genetically encoded probes (Pastor-Flores et al., 2020), will be required to further characterize this phenomenon.

Tracking the *in vivo* dynamics of oxidative thiol modulations is central to understating the role of redox regulation in adjusting metabolic activity. Yoshida et al., (2014) explored the diurnal redox dynamics of the CBC enzymes, FBPase and SBPase, and showed a change from fully oxidized to an almost fully reduced state of FBPase during a gradual increase in light intensity from dark to 350 µmol m^{-2} s^{-1}. Intriguingly, the observed light range in which FBPase reduction occurred, matched the range of light-induced changes in 2-Cys redox signaling, as observed either by direct measurements of the 2-Cys Prx redox state or by using the roGFP2-PrxΔC_R (Fig. 1F&4B). Considering the sensitivity of FBPase to 2-Cys Prx-mediated oxidation (Yoshida et al., 2018), these results suggest that the reductive and oxidative pathways are interconnected in regulating carbon assimilation rates under low- and moderate-light conditions.

Due to the heterogeneous organization and spatial arrangement of crop canopy, leaves lower in the canopy experience sporadic high light, scattered with low-light levels of variable durations. Given the dominant role of redox signaling at low to moderate light intensities, the level of activation and deactivation of CBC enzymes in lower leaves will vary throughout the day with both the reductive and oxidizing signal shaping the rate of carbon assimilation rate, defining the contribution of these leaves to the total carbon assimilation rates (Sassenrath-Cole and Pearcy, 1994). Concerning deactivation of CBC enzymes by oxidative signals, the inherent redox changes that stimulate the activation of CBC enzymes and serve to link carbon fixation to electron transport activity and energy flux also govern limitation to optimal canopy assimilation under fluctuating light intensities. Given the role of 2-Cys Prx in deactivating CBC enzyme activity, our data suggest

that the roGFP2-PrxΔC_R probe can serve to estimate the degree of limitation of photosynthesis imposed by oxidative signals in plants.

To conclude, this study employed a 2-Cys Prx-based probe to systematically track oxidative signals emanating from the PETC into target proteins. Our results suggest that the chl-roGFP2-PrxΔC_R probe accurately reports on changes in photosynthetically produced oxidative signals, through quantifiable fluorescent signals. The proposed biosensor has the potential to provide fundamental insights into the role of redox signaling in light acclimation of higher plants, expanding the current set of tools to nondestructively monitor photosynthetic parameters.

Material and Methods

Plant growth conditions and treatment

Arabidopsis thaliana ecotype Col-0 plants were grown in a greenhouse under a 16/8 h light/dark cycle. Immunoassay, redox imaging and thiol labelling experiments were performed on whole, three-week-old *Arabidopsis* plants. For the 3-(3,4-dichlorophenyl)-1,1-dimethylurea (DCMU) treatment, three-week-old plants were sprayed with 150µM DCMU (D2425-100G, Sigma) in the dark phase, 1 hour before the onset of the light period.

Construction of roGFP2-PrxΔC_R and PrxΔC_R-roGFP2 probes

Both fusion probes (roGFP2-PrxΔC_R and PrxΔC_R-roGFP2) were synthesized with codons optimized for *Arabidopsis* expression (Genewiz). Chloroplast targeting was achieved by using the 2-Cys peroxiredoxin A signal peptide. The genetically fused sequences were cloned into the plant cloning vector pART7, using the XhoI and HindIII restriction enzymes. The whole construct, including the CaMV 35S promoter and ocs terminator, was then cloned into the binary vector pART27, using the NotI restriction enzyme. The pART27 plasmids containing the roGFP2-PrxΔC_R and PrxΔC_R-roGFP2 probe constructs, were transformed into GV3101 *Agrobacterium tumefaciens*. Transformation of Arabidopsis thaliana (Columbia, Col-0) was then performed by floral dip (Clough and Bent, 1998). Transformant lines were selected based on kanamycin resistance and the chl-roGFP2 fluorescence signal.

Determination of 2-Cys Prx redox state by immunolabeling

NEM labeling. Protein extracts were prepared in the presence of 1 ml cold 10% trichloroacetic acid (TCA) (dissolved in water) to retain the *in vivo* thiol oxidation status of proteins. Proteins were precipitated for 30 min on ice, in the dark, and centrifuged at 19,000 xg for 20 min, at 4°C. The pellet was then washed four times with 100% cold acetone. After removal of the residual acetone, the pellet was resuspended in urea buffer (8M urea, 100mM 4-(2-hydroxyethyl)-1-piperazineethanesulfonic acid (HEPES) (pH 7.2), 1mM EDTA, 2% (w/v) SDS, protease inhibitors cocktail (PI) (Calbiochem) and 100mM N-ethylmaleimide (NEM) (E3876, Sigma)) dissolved in ethanol. Samples were then incubated for 30 min, at room temperature, followed by centrifugation (19,000 xg, 20 min, 4°C) and washed (4 times) with 100% cold acetone. The dry pellets were resuspended in urea buffer without NEM. The sample buffer (x3) contained 150mM Tris-HCl, pH 6.8, 6% (w/v) SDS, 30% glycerol and 0.3% pyronin Y. Gel fractionation was carried out without a reducing agent, on a precast 4–15% polyacrylamide gel. Fractionated proteins were transferred to a polyvinylidene fluoride membrane (Bio-Rad), using the Trans-Blot Turbo Transfer System (Bio-Rad) with Trans-Blot Turbo Midi Transfer Packs. The membrane was incubated with anti-PRX antibodies (1:1,000) (kindly provided by Prof. Avichai Danon) or an anti-peroxiredoxin-SO_3 antibody (Abcam, ab16830, 1:2000), both followed by anti-rabbit horseradish peroxidase (HRP)-conjugated IgG (1:20,000) (Agrisera). Chemiluminescence was detected using the Advanced Molecular Imager HT (Spectral Ami-HT, Spectral Instruments Imaging, LLC., USA).

mPEG labeling

Protein extract was prepared, using a hand homogenizer, in 1ml cold 10% trichloroacetic acid (TCA) (dissolved in water) to retain the *in vivo* thiol oxidation status of proteins. Proteins were precipitated for 30 min, on ice, in the dark, and then centrifuged at 19,000 xg for 20 min at 4°C. The pellet was washed four times with 100% cold acetone, after which, residual acetone was removed and the pellet was resuspended in urea buffer with NEM. The samples were then incubated for 30 min at room temperature. Samples were then reduced by addition of 100mM DTT (60 min, room temperature). TCA (10%) was then added and samples were precipitated for 30 min, on ice, in the dark. The TCA-treated extracts were then centrifuged at 19,000 xg, 4°C for 20 min, supernatants were removed and the pellets were washed three times with 100% acetone. The dry pellets were resuspended in urea buffer containing 10mM methoxy-polyethylene glycol

maleimide (mPEG, MW 5000 g/mol, Sigma), and incubated at 28 °C for 2 h. The reaction was stopped by adding an equal volume of sample buffer containing 50 mM DTT. Samples were then separated by 10% Tricine–SDS–PAGE and then transferred to a polyvinylidene fluoride membrane (Bio-Rad) under the same conditions described above. The membrane was incubated with anti-PRX antibodies (1:1,000) and then with anti-rabbit HRP-conjugated IgG (1:20,000).

Probe detection using western analysis

Experiments were performed on 10-day-old seedlings. Whole-plant contents were extracted with extraction buffer (20 mM Tris, pH 8.0, 1 mM EDTA, and 50 mM NaCl), and then centrifuged at 19,000 xg, for 20 min, at 4°C. Gel fractionation of 100 µg extracted protein was carried out by reducing 10% SDS-PAGE. Fractionated proteins were then transferred onto a polyvinylidene fluoride membrane, which was then incubated with anti-PRX antibodies (1:1,000) or anti-GFP (abcam) antibodies (1:5,000), and then with anti-rabbit HRP-conjugated IgG (1:20,000).

Confocal microscopy

Confocal microscopy analysis was carried out on 2-week-old transgenic roGFP2, roGFP2-PrxΔC_R and PrxΔC_R-roGFP2-expressing plants. Images were captured with a Leica TCS SP8 confocal system (Leica Microsystems) and the LAS X Life Science Software, while using a HC PL APO ×40/1.10 objective. To capture chl-roGFP2 fluorescence, samples were excited at 488 nm and emission was measured at 500–520 nm. For chlorophyll fluorescence, excitation was at 488 nm and emission was at 670 nm. Merged images were generated using Fiji (Image 1.A) software.

roGFP2 fluorescence measurements and analysis

Redox imaging was performed on three-week-old transgenic chl-roGFP2 and roGFP2-PrxΔC_R-expressing plants. Whole-plant roGFP2 fluorescence was detected using an Advanced Molecular Imager HT, and images were taken using the AMIview software. For roGFP fluorescence images, excitation was at 465nm (reduction) and 405nm (oxidation), followed by emission at 510nm. Chlorophyll fluorescence, which was used to select plant tissue pixels, was measured following excitation at 405 and emission at 670. For each probe, images were taken under the same settings of LED intensities and exposure time. Ratiometric images were created by dividing, pixel by pixel, the 405 nm image by the 465 nm image, and displaying in false colors.

Images were processed using a custom-written Matlab script. For calibration of the probe response, detached plants were immersed in 0.5M H_2O_2 or 100 mM DTT, and ratiometric images for fully oxidized and fully reduced states, respectively, were obtained.

Daily roGFP2 fluorescence was measured (Rosenwasser et al., 2010) using a Tecan Spark® multimode microplate reader. For both probes (roGFP2 and roGFP2-PrxΔC_R), roGFP fluorescence was measured using excitation at 485nm/20 (reduction) and 400nm/20 (oxidation), followed by emission at 520nm/10; gain values were adjusted to avoid signal saturation. For chlorophyll detection, 400nm/20 was applied for excitation, followed by 670nm/40 for emission. For automatic detection of chl-roGFP2 signals, 10-day-old plants expressing the roGFP2-based probes or wild type plants were transferred to solid peat plugs in 12-well plates. The plates were placed in a growth chamber (Fytoscope FS-SI-4600, Photon Systems Instruments, Czech Republic) under normal growth conditions for another 5 days before the start of the experiment. An automated robot (KiNEDx KX.01467, paa automations, Hampshire, UK) controlled by a self-compiled program (Overlord™, paa automations), inserted the plates into the plate reader to measure chl-roGFP2 fluorescence. For the plate-reader analysis, a 9-by-9-pixel matrix was formed for each well. Chlorophyll fluorescence was detected to create a chlorophyll mask, which was then used to choose pixels that returned a positive chlorophyll fluorescence signal, and only those pixels were considered for the roGFP analysis. The average signals of non-fluorescent plants (WT) was calculated, and the values were deducted from the values detected in the chl-roGFP2 fluorescence analysis. To determine sensor OxD, detached roGFP-based probe-expressing and WT plants were immersed in 0.5M H_2O_2 or 100 mM DTT and fluorescence was measured. roGFP2 OxD was calculated based on the fluorescence signal according to Equation (Meyer et al., 2007).

Equation 1:

$$OxD_{roGFP2} = \frac{R - R_{\mathrm{red}}}{(I_{485\mathrm{min}}/I_{485\mathrm{max}})(R_{\mathrm{ox}} - R) + (R - R_{\mathrm{red}})}$$

where R represents the ratio (400/485) at each point in the experiment, R_{red} represents the ratio under fully reduced conditions, R_{ox} represents the ratio under fully oxidized conditions, $I485_{min}$ represents the fluorescence emitted at 520 nm when excited at 485 nm under fully oxidized conditions and $I485_{max}$ represents the fluorescence emitted at 520 nm when excited at 485 nm under fully reduced conditions.

A self-written Matlab script was used to analyze the many files that contained the measurements of each experiment. In addition, experimental metadata such as plant lines, light irradiance, temperature, relative humidity and CO_2 concentration were also collected and added to the output file.

Author contributions: N.L. and S.R. conceived and designed the research. N.L., I.N., G.G., M.H., and S.R. performed the research. N.L., M.H., and S.R. analyzed the data. N.L., and S.R. wrote the manuscript.

Acknowledgments: We thank Avihai Danon for his critical comments on the manuscript and for kindly providing us the anti-2-Cys Prx antibody. We thank Bruce Morgan for his kindly help in initiating this project. This research was supported by the Israel Science Foundation (grant No. 826/17 and No. 827/17).

References

Apel, K. and Hirt, H. (2004). REACTIVE OXYGEN SPECIES: metabolism, oxidative stress, and signal transduction. Annu. Rev. Plant Biol. **55**: 373–399.

Asada, K. (2006). Production and scavenging of reactive oxygen species in chloroplasts and their functions. Plant Physiol. **141**: 391 LP – 396.

Awad, J., Stotz, H.U., Fekete, A., Krischke, M., Engert, C., Havaux, M., Berger, S., and Mueller, M.J. (2015). 2-Cysteine peroxiredoxins and thylakoid ascorbate peroxidase create a water-water cycle that is essential to protect the photosynthetic apparatus under high light stress conditions. Plant Physiol. **167**: 1592 LP – 1603.

Buchanan, B.B. and Balmer, Y. (2005). REDOX REGULATION: A broadening horizon. Annu. Rev. Plant Biol. **56**: 187–220.

Cerveau, D., Kraut, A., Stotz, H.U., Mueller, M.J., Couté, Y., and Rey, P. (2016). Characterization of the Arabidopsis thaliana 2-Cys peroxiredoxin interactome. Plant Sci. **252**: 30–41.

Collin, V., Issakidis-Bourguet, E., Marchand, C., Hirasawa, M., Lancelin, J.-M., Knaff, D.B., and Miginiac-Maslow, M. (2003). The Arabidopsis Plastidial Thioredoxins: new functions and new insights into specificity. J. Biol. Chem. **278**: 23747–23752.

Dangoor, I., Peled-Zehavi, H., Wittenberg, G., and Danon, A. (2012). A chloroplast light-regulated oxidative sensor for moderate light intensity in Arabidopsis. Plant Cell **24**: 1894–906.

Dietz, K.-J. (2016). Thiol-based peroxidases and ascorbate peroxidases: why plants rely on multiple peroxidase systems in the photosynthesizing chloroplast? Mol. Cells **39**: 20–5.

Dietz, K.-J., Jacob, S., Oelze, M.-L., Laxa, M., Tognetti, V., de Miranda, S.M.N., Baier, M., and Finkemeier, I. (2006). The function of peroxiredoxins in plant organelle redox metabolism. J. Exp. Bot. **57**: 1697–1709.

Dietz, K.-J. and Pfannschmidt, T. (2011). Novel regulators in photosynthetic redox control of plant metabolism and gene expression. Plant Physiol. **155**: 1477–85.

Dooley, C.T., Dore, T.M., Hanson, G.T., Jackson, W.C., Remington, S.J., and Tsien, R.Y. (2004). Imaging dynamic redox changes in mammalian cells with green fluorescent protein indicators. J. Biol. Chem. **279**: 22284–22293.

Eliyahu, E., Rog, I., Inbal, D., and Danon, A. (2015). ACHT4-driven oxidation of APS1 attenuates starch synthesis under low light intensity in *Arabidopsis* plants. Proc. Natl. Acad. Sci. **112**: 12876 LP – 12881.

Foyer, C.H. and Noctor, G. (2009). Redox regulation in photosynthetic organisms. Regulation **11**: 861–905.

Gutscher, M., Pauleau, A.-L., Marty, L., Brach, T., Wabnitz, G.H., Samstag, Y., Meyer, A.J., and Dick, T.P. (2008). Real-time imaging of the intracellular glutathione redox potential. Nat. Methods **5**: 553–559.

Gutscher, M., Sobotta, M.C., Wabnitz, G.H., Ballikaya, S., Meyer, A.J., Samstag, Y., and Dick, T.P. (2009). Proximity-based protein thiol oxidation by H_2O_2-scavenging peroxidases. J. Biol. Chem. **284**: 31532–31540.

Haber, Z. and Rosenwasser, S. (2020). Resolving the dynamics of photosynthetically produced ROS by high-resolution monitoring of chloroplastic E_{GSH} in *Arabidopsis*. bioRxiv: 2020.03.04.976092.

Hanson, G.T., Aggeler, R., Oglesbee, D., Cannon, M., Capaldi, R.A., Tsien, R.Y., and Remington, S.J. (2004). Investigating mitochondrial redox potential with redox-sensitive green fluorescent protein indicators. J. Biol. Chem. **279**: 13044–13053.

Jiang, K., Schwarzer, C., Lally, E., Zhang, S., Ruzin, S., Machen, T., Remington, S.J., and Feldman, L. (2006). Expression and characterization of a redox-sensing green fluorescent protein (Reduction-Oxidation-Sensitive Green Fluorescent Protein) in *Arabidopsis*. Plant Physiol. **141**: 397 LP – 403.

König, J., Baier, M., Horling, F., Kahmann, U., Harris, G., Schürmann, P., and Dietz, K.-J. (2002). The plant-specific function of 2-Cys peroxiredoxin-mediated detoxification of peroxides in the redox-hierarchy of photosynthetic electron flux. Proc. Natl. Acad. Sci. **99**: 5738 LP – 5743.

Mehler, A.H. (1951). Studies on reactions of illuminated chloroplasts: I. Mechanism of the reduction of oxygen and other hill reagents. Arch. Biochem. Biophys. **33**: 65–77.

Meyer, a J. and Dick, T.P. (2010). Fluorescent protein-based redox probes. Antioxid Redox Signal **13**: 621–650.

Meyer, A.J., Brach, T., Marty, L., Kreye, S., Rouhier, N., Jacquot, J.-P., and Hell, R. (2007). Redox-sensitive GFP in Arabidopsis thaliana is a quantitative biosensor for the redox potential of the cellular glutathione redox buffer. Plant J. **52**: 973–986.

Mittler, R., Vanderauwera, S., Gollery, M., and Van Breusegem, F. (2004). Reactive oxygen gene network of plants. Trends Plant Sci. **9**: 490–498.

Morgan, B., Van Laer, K., Owusu, T.N.E., Ezeriņa, D., Pastor-Flores, D., Amponsah, P.S., Tursch, A., and Dick, T.P. (2016). Real-time monitoring of basal H_2O_2 levels with peroxiredoxin-based probes. Nat. Chem. Biol. **12**: 437–443.

Mullineaux, P.M., Exposito-Rodriguez, M., Laissue, P.P., and Smirnoff, N. (2018). ROS-dependent signalling pathways in plants and algae exposed to high light: Comparisons with other eukaryotes. Free Radic. Biol. Med. **122**: 52–64.

Nelson, K.J., Perkins, A., Van Swearingen, A.E.D., Hartman, S., Brereton, A.E., Parsonage, D., Salsbury, F.R., Karplus, P.A., and Poole, L.B. (2017). Experimentally dissecting the origins of peroxiredoxin catalysis. Antioxid. Redox Signal. **28**: 521–536.

Niemeyer, J., Scheuring, D., Oestreicher, J., Morgan, B., and Schroda, M. (2020). Real-time monitoring of subcellular H_2O_2 distribution in *Chlamydomonas reinhardtii*. bioRxiv: 2020.11.13.382085.

Nietzel, T. et al. (2019). The fluorescent protein sensor roGFP2-Orp1 monitors in vivo H_2O_2 and

thiol redox integration and elucidates intracellular H_2O_2 dynamics during elicitor-induced oxidative burst in Arabidopsis. New Phytol. **221**: 1649–1664.

Ojeda, V., Pérez-Ruiz, J.M., and Cejudo, F.J. (2018). 2-Cys peroxiredoxins participate in the oxidation of chloroplast enzymes in the dark. Mol. Plant **11**: 1377–1388.

Pastor-Flores, D., Talwar, D., Pedre, B., and Dick, T.P. (2020). Real-time monitoring of peroxiredoxin oligomerization dynamics in living cells. Proc. Natl. Acad. Sci. **117**: 16313 LP – 16323.

Pérez-Ruiz, J.M. and Cejudo, F.J. (2009). A proposed reaction mechanism for rice NADPH thioredoxin reductase C, an enzyme with protein disulfide reductase activity. FEBS Lett. **583**: 1399–1402.

Pérez-Ruiz, J.M., Naranjo, B., Ojeda, V., Guinea, M., and Cejudo, F.J. (2017). NTRC-dependent redox balance of 2-Cys peroxiredoxins is needed for optimal function of the photosynthetic apparatus. Proc. Natl. Acad. Sci. **114**: 12069 LP – 12074.

Pulido, P., Spínola, M.C., Kirchsteiger, K., Guinea, M., Pascual, M.B., Sahrawy, M., Sandalio, L.M., Dietz, K.-J., González, M., and Cejudo, F.J. (2010). Functional analysis of the pathways for 2-Cys peroxiredoxin reduction in Arabidopsis thaliana chloroplasts. J. Exp. Bot. **61**: 4043–4054.

Rizhsky, L., Liang, H., and Mittler, R. (2003). The water-water cycle is essential for chloroplast protection in the absence of stress. J. Biol. Chem. **278**: 38921–38925.

Sassenrath-Cole, G.F. and Pearcy, R.W. (1994). Regulation of Photosynthetic Induction State by the Magnitude and Duration of Low Light Exposure. Plant Physiol. **105**: 1115 LP – 1123.

Scheibe, R. and Dietz, K.-J. (2012). Reduction–oxidation network for flexible adjustment of cellular metabolism in photoautotrophic cells. Plant. Cell Environ. **35**: 202–216.

Schürmann, P. and Buchanan, B.B. (2008). The Ferredoxin/Thioredoxin system of oxygenic photosynthesis. Antioxid. Redox Signal. **10**: 1235–1274.

Serrato, A.J., Pérez-Ruiz, J.M., Spínola, M.C., and Cejudo, F.J. (2004). A novel NADPH thioredoxin reductase, localized in the chloroplast, which deficiency causes hypersensitivity to abiotic stress in Arabidopsis thaliana. J. Biol. Chem. **279**: 43821–43827.

Smirnoff, N. and Arnaud, D. (2019). Hydrogen peroxide metabolism and functions in plants. New Phytol. **221**: 1197–1214.

Stöcker, S., Van Laer, K., Mijuskovic, A., and Dick, T.P. (2017). The conundrum of hydrogen peroxide signaling and the emerging role of peroxiredoxins as redox relay hubs. Antioxid. Redox Signal. **28**: 558–573.

Vaseghi, M.-J., Chibani, K., Telman, W., Liebthal, M.F., Gerken, M., Schnitzer, H., Mueller, S.M., and Dietz, K.-J. (2018). The chloroplast 2-cysteine peroxiredoxin functions as thioredoxin oxidase in redox regulation of chloroplast metabolism. Elife **7**: e38194.

Wolf, B.-C., Isaacson, T., Tiwari, V., Dangoor, I., Mufkadi, S., and Danon, A. (2020). Redox

regulation of PGRL1 at the onset of low light intensity. Plant J. **103**: 715–725.

Yoshida, K., Hara, A., Sugiura, K., Fukaya, Y., and Hisabori, T. (2018). Thioredoxin-like2/2-Cys peroxiredoxin redox cascade supports oxidative thiol modulation in chloroplasts. Proc. Natl. Acad. Sci. **115**: E8296 LP-E8304.

Yoshida, K., Matsuoka, Y., Hara, S., Konno, H., and Hisabori, T. (2014). Distinct redox behaviors of chloroplast thiol enzymes and their relationships with photosynthetic electron transport in arabidopsis thaliana. Plant Cell Physiol. **55**: 1415–1425.